A SIMPLE MODEL FOR THE GENERATION OF ULTRA-SHORT RADIATION PULSES

L.T. Campbell and B.W.J. M[c]Neil
SUPA, Department of Physics, University of Strathclyde, Glasgow, UK

Abstract

A method for generating a single broadband radiation pulse from a strongly chirped electron pulse is described. The evolution of the chirped electron pulse in an undulator may generate a pulse of coherent spontaneous radiation of shorter duration than the FEL cooperation length. An analytic expression for the emitted radiation pulse is derived and compared with numerical simulation.

INTRODUCTION

Free Electron Lasers based on the SASE mechanism produce intense, uncorrelated radiation pulses of width approximately equal to the FEL cooperation length, l_c [1]. For sufficiently short electron pulses only one single pulse may be emitted. However, such a mode of operation results in output pulses that contain significant temporal jitter. Other methods are being considered to improve the temporal coherence, and to further reduce the temporal width of the radiation pulses [2].

The method discussed here predicts emission of a single radiation pulse of width $< l_c$ from a short, strongly-chirped electron beam evolving in an undulator. The method is described from a general perspective without reference to any specific electron beam source.

A sufficiently strong negative chirp in an electron pulse will cause the pulse to shorten in longitudinal phase space when propogating in an undulator as shown in Fig. 1. After a sufficient propagation distance, the pulse length will come to a minimum, the energy chirp will then become positive and the pulse will start to lengthen.

If the electron pulse length evolves to the order of a resonant FEL wavelength λ_r, it will generate a short pulse of coherent radiation. This coherent spontaneous emission may occur for a number of undulator periods dependent upon the magnitude of the chirp and the length of the electron pulse. For example, for a stronger chirp will cause thee electron pulse to radiate coherently for fewer undulator periods, resulting in a shorter radiation pulse of broader bandwidth.

This is not an FEL effect, rather, it is a coherent effect arising purely from the linear evolution of the electron beam due to the chirp. Nevertheless, an unaveraged system of FEL equations is used to describe the effect, as it is capable of describing both the evolution of the longitudinal shape of the electron pulse, and the consequent emission of CSE from the short electron pulse of length $< \lambda_r$, neither of which can be described using an averaged set of undulator/FEL equations.

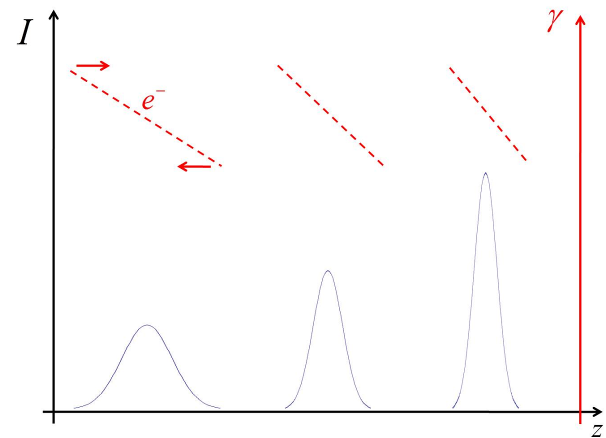

Figure 1: Schematic of the evolution of short negatively chirped electron pulse propagating through an undulator showing the current I and scaled energy γ.

Here, a 1D analytic solution of the expected coherent radiation output from such a chirped electron pulse is derived and compared with both a 1D and 3D numerical simulation using the unaveraged FEL code Puffin [3].

ANALYTIC SOLUTION

An analytic solution is derived from the un-averaged system of FEL equations presented of [4]. These equations are identical to those of the code Puffin [3] in the 1D Compton limit. The electrons are assumed uncoupled from the radiation so that only the wave equation need be solved:

$$\left(\frac{\partial}{\partial \bar{z}} + \frac{\partial}{\partial \bar{z}_1}\right) A(\bar{z}, \bar{z}_1) = \frac{1}{\bar{n}_{p\|}} \sum_{j=1}^{N} e^{-i\frac{\bar{z}_1}{2\rho}} \delta(\bar{z}_1 - \bar{z}_{1j}), \quad (1)$$

where the scaling of [4] has been used. As in [4], the source term can be put into a more convenient functional form by discretising $\bar{z}_1$ into intervals of width $\Delta\bar{z}_1 << 4\pi\rho$, i.e. much less than a radiation wavelength. In this way, the source term of (1) becomes a sum over discrete intervals:

$$\sum_{n=-\infty}^{\infty} \chi_n(\bar{z})\, e^{-i\frac{\bar{z}_1}{2\rho}} \delta(\bar{z}_1 - \bar{z}_{1n}) \Delta\bar{z}_1, \quad (2)$$

where: $\chi_n(\bar{z}) \equiv I_n(\bar{z})/I_{pk}$ is the current in the n-th interval scaled with respect to the peak current of the electron pulse at the beginning of the undulator, $\bar{z} = 0$. The solution proceeds by then taking the unitary Fourier transform,

ISBN 978-3-95450-123-6

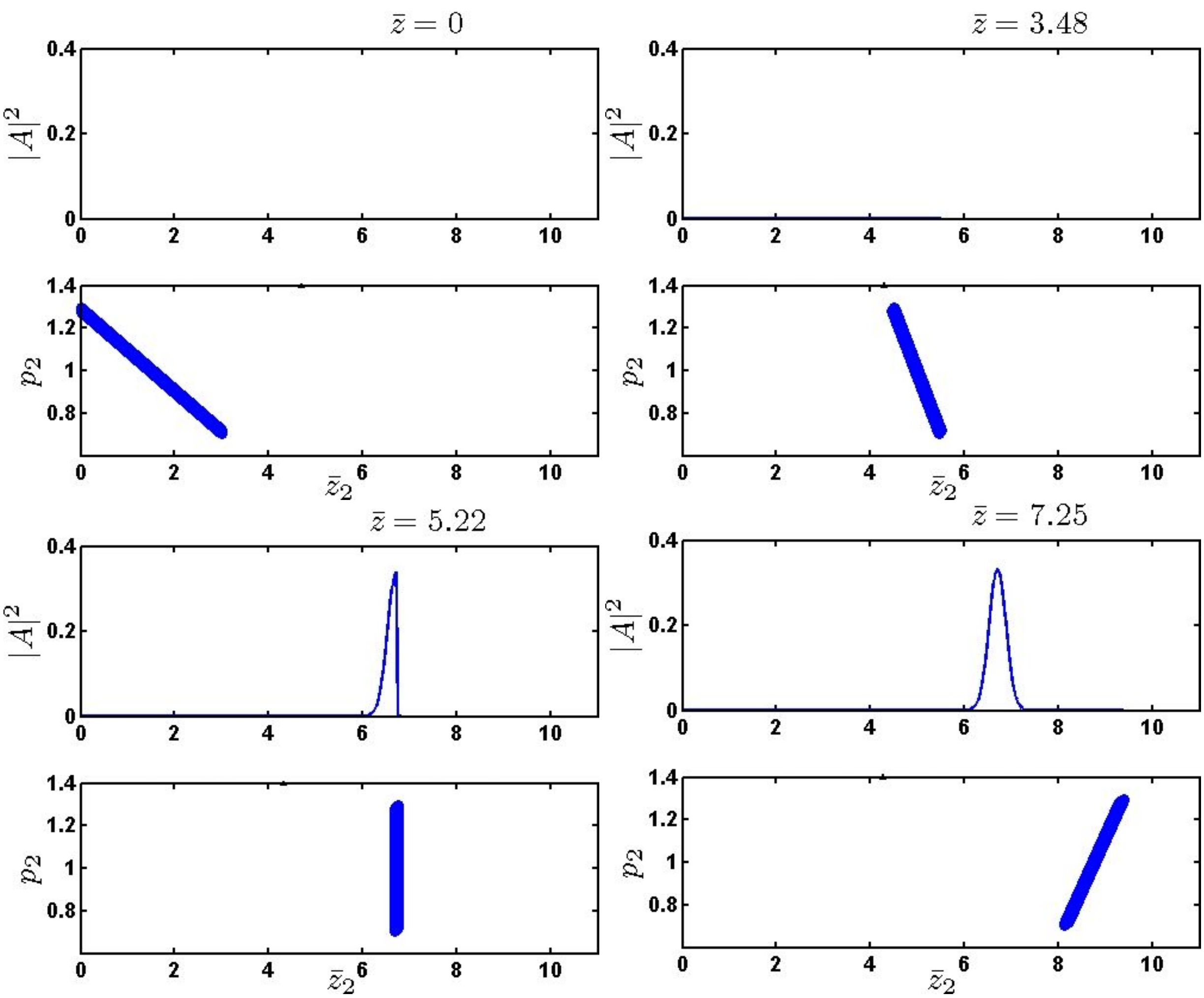

Figure 2: These 8 plots show the intensity and electron beam phase space at 4 different propagation distances. The initial chirp in the plot at $\bar{z} = 0$ in the top left causes the electron pulse to compress and then decompress. When it is bunched to a length in $\bar{z}_2$ of $\lesssim 4\pi\rho$ (that is to say, less than a resonant radiation wavelength) it generates a single coherent spike in intensity.

$F_{\bar{\omega}}\{X(\bar{z}, \bar{z}_1)\} = \tilde{X}(\bar{z}, \bar{\omega})$, of (1), redefining the radiation field envelope so that $A'(\bar{z}, \bar{\omega}) = \tilde{A}(\bar{z}, \bar{\omega})e^{i\bar{\omega}\bar{z}}$ and taking the limit $\Delta\bar{z}_1 \to 0$ in the source term to obtain:

$$\frac{\partial A'(\bar{z}, \bar{\omega})}{\partial \bar{z}} = \sqrt{2\pi} e^{i\bar{\omega}\bar{z}} \tilde{\chi}(\bar{z}, \bar{\omega}'), \qquad (3)$$

where $\bar{\omega}' \equiv \bar{\omega} + 1/2\rho$. Under the assumptions of [4], this is a general equation for the wave envelope for a given scaled current $\chi(\bar{z}, \bar{z}_1)$.

It is now assumed that the electron current has a Gaussian distribution with a linear, negative energy chirp and in scaled form is given by:

$$\chi(\bar{z}, \bar{z}_1) = \frac{\sigma_0}{\sigma(\bar{z})} \exp\left(\frac{-\bar{z}_1^2}{2\sigma^2(\bar{z})}\right) \qquad (4)$$

where $\sigma(\bar{z}) = \sqrt{\sigma_0^2 (1 + g_0\bar{z})^2 + \sigma_r^2}$ is the $\bar{z}$ dependent width due to a linear scaled energy chirp. The chirp is defined in electron phase space at the start of the undulator by: $p_0(\bar{z}_1) \equiv (\gamma(\bar{z}_1) - \gamma_r)/\rho\gamma_r = g_0\bar{z}_1$ where g_0 is the initial chirp gradient in $\bar{z}_1$. Hence, the the range of electron energies in the pulse is determined by the product $g_0\sigma_0$. Here it is assumed $g_0 < 0$. The constant σ_r describes a minimum residual width of the pulse when $g_0\bar{z} = -1$.

This evolution of the electron pulse as a function of $\bar{z}$ allows the field equation (3) to be integrated over $-\infty < \bar{z} < \infty$ to obtain an analytic solution for the field. To enable a solution, a transform to a new independent variable $\hat{z} = 1 + g_0\bar{z}$ is made so that $g_0 = 0$ is not allowed. Note also, that the evolution as a function of $\bar{z}$ is not given, only the result of the electron emission in an undulator of sufficient length $\bar{z} \gg |g_0|^{-1}$. The solution is obtained in Fourier space, and the final expression for the envelope as a function of $f = \omega/\omega_r$ may be written as:

$$\tilde{A}(f) = \frac{4\pi\rho}{f} \exp\left(-i\frac{f-1}{2\rho g_0} - \frac{f^2\sigma_i^2}{8\rho^2} - \frac{(f-1)^2}{2g_0^2\sigma_0^2 f^2}\right) \qquad (5)$$

It is clear from the final term in the exponent of the expo-

ISBN 978-3-95450-123-6

nential term that the greater the total energy range within the electron pulse, as defined by $g_0\sigma_0$, the broader the radiation spectrum and the shorter the radiation pulse generated. In what follows, both 1D and 3D simulation are presented and compared with the above analysis.

SIMULATIONS

The non-averaged FEL simulation code Puffin [3] was used to simulate typical output from an helical undulator using the following parameters: $\rho = 8 \times 10^{-3}$, $\bar{a}_u = 1.5$, $\gamma = 707$ and $\lambda_w = 1.5$cm. An electron beam energy chirp of $g_0 = -0.192$ was applied to a Gaussian current distribution with scaled rms width of $\sigma_0 = 0.333$. An homogeneous energy spread of $\sigma_\gamma/\gamma = 0.17\rho$ was also used.

In what follows, the scaled units of [3] are used. The main difference from the results above derived from (1) is a change from the independent variable $\bar{z}_1$ to $\bar{z}_2 = \bar{z}-\bar{z}_1$. A resonant electron would propagate along $\bar{z}_1$ =constant i.e. $\bar{z}_1$ measures distance in units of l_c in the resonant electron rest-frame away from the *tail* of the electron pulse. However, a radiation wavefront propagates along $\bar{z}_2$=constant and $\bar{z}_2$ measures distance in units of l_c in the light rest-frame away from the *head* of the light pulse. Note that p_{2j} is the rate of change of the j-th electron's position in $\bar{z}_2$, so that a larger values of p_{2j} means the electron will propagate faster away from the head of the light pulse - i.e. larger p_{2j} means a lower electron energy.

The results of a 1D simulation using the above parameters and shown in Fig. 2 which plots the scaled radiation intensity and the evolution in $(\bar{z}_2, p_2)$ phase space of the electron bunch as it propagates through the undulator. (Note that in the 1D limit, $|A|^2$ is the scaled intensity, not power, generated by an electron beam of uniform transverse density.) Electron bunch compression and decompression due to the energy chirp is seen as the interaction progresses. As the length of the electron pulse approaches that of the resonant radiation wavelength ($4\pi\rho \approx 0.1$), it starts to radiate strongly and coherently. This is seen in the phase space plot at $\bar{z} = 5.22$ which shows the compressed electron bunch emitting a coherent radiation spike in the corresponding intensity plot. Further propagation begins to de-bunch the electrons and the coherent emission reduces, so forming the short radiation pulse. Note that the final radiation pulse width, from the intensity plot at $\bar{z} = 7.25$ of Fig. 2, is slightly less than a cooperation length. The radiation pulse width may be significantly less than one cooperation length, which is smaller than pulse widths produced by the FEL process in SASE.

The radiation intensity spectrum was calculated using a numerical Fourier transform and is plotted in Fig. 3. This spectrum is in very good agreement with the analytical solution of equation (5).

A 3D simulation using the same parameters as above was carried out. A scaled emittance of $\bar{\epsilon} = 4\pi\epsilon/\lambda_r = 1.6$ was used and the beam radius matched to the undulator using natural focussing. This gives an effective energy spread,

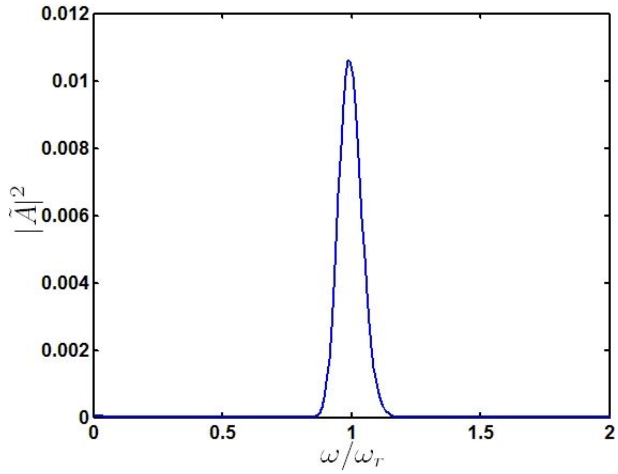

Figure 3: The intensity spectrum $|\tilde{A}|^2$ plotted as a function of scaled frequency $f = \omega/\omega_r$ at $\bar{z} = 7.6676$ as shown in Fig. 2.

from [5], of $\sigma_\epsilon = 0.00064$, which is very small compared to the homogeneous energy spread as used in the 1D simulation above. The betatron wavelength in units of $\bar{z}$ is $\bar{\lambda}_\beta = 4\sqrt{2}\pi\gamma\rho/\bar{a}_u = 67.01$, and the Rayleigh length of the resonant wavelength for the matched beam radius, again in units of $\bar{z}$, is $\bar{z}_R = \bar{\epsilon}\bar{\lambda}_\beta/4\pi = 8.532$ [3], both of which are relatively large with respect to the FEL gain length. With these parameters it may be expected, and as is shown below, that diffraction and emittance effects are relatively small so that the results will not deviate significantly from the 1D simulation of above.

From the 3D simulations, the transverse plot of the scaled intensity at $\bar{z} = 7.6676$ and $\bar{z}_2 = 7.0456$, close to the coherently radiated peak is plotted in Fig. 4. A sharp peak is seen on-axis at $(\bar{x}, \bar{y}) \approx (0, 0)$ where the electron pulse is propagating. The scaled power $|A|^2$ is calculated by integrating the scaled intensity over the transverse region of the simulation and is plotted in Fig. 5 as a function of $\bar{z}_2$. As with the 1D case, the sharp peak in the power in the region $6 \leq \bar{z}_2 \leq 7$ indicates where the electron beam became strongly bunched and emitted a strong coherent pulse.

The scaled spectral intensity was calculated from the data along the center of the transverse plane at $(\bar{x}, \bar{y}) \approx (0, 0)$ and is plotted in Fig. 6. It can be seen that the spectrum is in good agreement with that of the analytical solution and the 1D simulation of Fig. 3. As expected from the calculated betatron wavelength and Rayleigh range above, the 3D effects have not significantly reduced the spectral intensity, and the emission of the radiation from the chirped pulse has not been significantly degraded.

CONCLUSIONS

Using a relatively simple 1D model, a method was described which appears capable of generating a single, intense, broad-bandwidth radiation pulse from a short

ISBN 978-3-95450-123-6

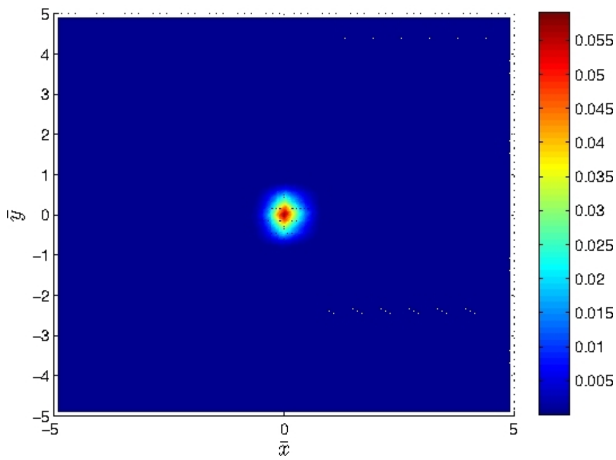

Figure 4: The transverse intensity profile near the peak at $\bar{z} = 7.6676$ and $\bar{z}_2 = 7.0456$ as shown in Fig. 5.

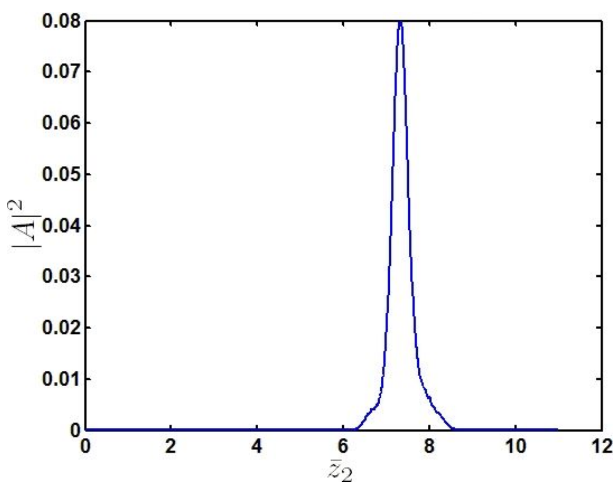

Figure 5: The scaled power $|A|^2$ is calculated by integrating the scaled intensity of Fig. 4 over the transverse area and is plotted as a function of $\bar{z}_2$ for $\bar{z} = 7.6676$.

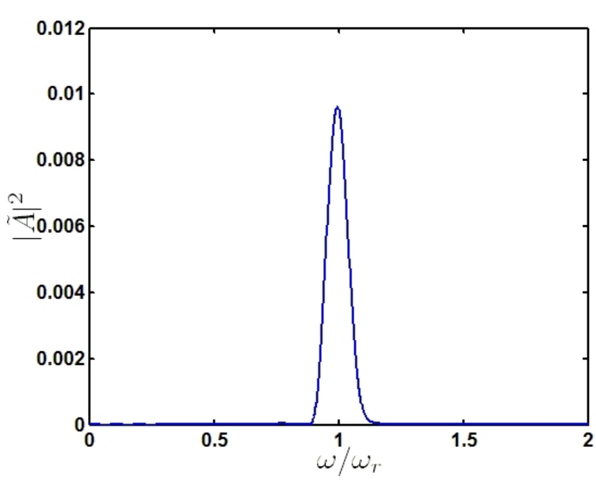

Figure 6: The spectral intensity calculated on-axis along the $\bar{z}_2$ axis at $\bar{z} = 7.6676$.

chirped electron pulse in an undulator. Analysis and simulations in both 1D and 3D using the unaveraged modelling of [3] show good agreement. It is noted that the gaussian pulse current used in the model is not best suited to generating strong coherent emission and other current profiles can be expected to generate more intense output.

REFERENCES

[1] R. Bonifacio, L. de Salvo, P. Pierini, N. Piovella and C. Pellegrini, Phys. Rev. Lett. **73**, 70 (1994)

[2] Brian W. J. McNeil and Neil R. Thompson, Nature Photon. **4**, 814 (2010)

[3] L.T. Campbell and B.W.J. McNeil, 'Puffin: A three dimensional, unaveraged Free Electron Laser simulation code', **MOPD12**, 34th International FEL Conference, Nara, Japan (2012)

[4] B.W.J. McNeil, M.W. Poole and G.R.M. Robb, Phys. Rev. ST-AB **6**, 070701 (2003)

[5] R. Bonifacio, L. De Salvo Souza and B.W.J. McNeil, Optics Comm, Vol 93, 179-185 (1992).

ISBN 978-3-95450-123-6